ISSN: 0067-2904

Inhibitory Effects of Iron Oxide Nanoparticles Biosynthesized by Prodigiosin Pigment Against Clinical Bacteria Isolates of *Pseudomonas aeruginosa*

Bakr A. Ahmed [1]*, Laith A. Yaaqoob
Biotechnology Department, College of Science, University of Baghdad, Baghdad, Iraq

Received: 25/6/2023 Accepted: 26/9/2023 Published: 30/11/2024

Abstract

The current study aimed to reveal the biosynthesis technique of Fe_2O_3 nanoparticles by using prodigiosin pigment production from *Serratia marcescens*. One hundred and twenty samples were obtained from burn and wound infections to isolate *Pseudomonas aeruginosa.* In addition, the optimum conditions for Fe_2O_3 nanoparticles biosynthesis were characterized via different methods, including ultraviolet-visible (UV-Vis), atomic force microscope (AFM), fourier transforms infrared (FT-IR) spectroscopy analysis, X-ray diffraction (XRD), and field emission scanning electron microscopy (FE-SEM). In particular, spherical shape particles were observed utilizing FE-SEM technique. In addition, the analysis of AFM revealed Fe_2O_3 NPs with an average diameter size of 50.73 nm. The influences of varied concentrations of iron nanoparticles (6.25, 25 ,12.5, 50, 100and 200 mg/ml) on a bacterial isolate of *Pseudomonas aeruginosa* were examined. The maximum inhibition zone of *P. aeruginosa* was 24 mm at a concentration of 200 mg/ml of Fe_2O_3 NPs, whereas the minimum inhibition zone were 10 mm located at 25 mg/ml Fe_2O_3 NPs concentrations.

Keywords*:* *Pseudomonas aeruginosa*, Iron oxide nanoparticles, *Serratia marcescens*, Antibacterial activity, Prodigiosin

التأثير المثبط لجسيمات أكسيد الحديد النانوية المُصنَّعة حيوياً بواسطة صبغة بروديجيوسين ضد العزلة السريرية لبكتيريا الزائفة الزنجارية

بكر عبد اللطيف احمد *، ليث احمد يعقوب
قسم تقنيات احيائية, كلية العلوم,جامعة بغداد,بغداد, العراق

الخلاصة

هدفت الدراسة الحالية إلى الكشف عن تقنية التخليق الحيوي لجسيمات الحديد النانوية Fe_2O_3 عن طريق إنتاج صبغة بروديجيوسين من *Serratia marcescens*. تم الحصول على 120 عينة من اصابات الحروق والجروح لعزل *Pseudomonas aeruginosa*. بالإضافة إلى ذلك، تم تمييز الظروف المثلى للتخليق الحيوي لجسيمات Fe_2O_3 النانوية عبر طرق مختلفة، بما في ذلك الأشعة فوق البنفسجية المرئية (UV–Vis)، مجهر القوة الذرية (AFM)، التحليل الطيفي للأشعة تحت الحمراء (FT–IR) ، وحيود الأشعة السينية (XRD) والمجهر الإلكتروني لمسح الانبعاث الميداني (FE–SEM). على وجه الخصوص، لوحظت

*Email: aljanabibaker897@gmail.com

جزيئات كروية الشكل باستخدام تقنية (FE−SEM). إضافة الى ذلك، كشف تحليل (AFM) ان الجسيمات النانوية تمتلك متوسط حجم قطر (50.73) نانوميتر. فحص تأثير تراكيز مختلفة من جسيمات الحديد النانوية (200، 100، 50، 25، 12.5، 6.25 ملغرام/مل) على عزلة بكتيريا *P. aeruginosa*. كانت اعلى منطقة تثبيط لبكتيريا *P. aeruginosa* هي 24 مليميتر وبتركيز 200 ملغرام/مل من جسيمات الحديد النانوية، بينما كانت ادنى منطقة تثبيط هي 10 مليميتر وبتركيز 25 ملغرام/مل من جسيمات الحديد النانوية.

كلمات مفتاحية: الزائفة الزنجارية، الجزيئات النانوية لاوكسيد الحديد، *Serratia marcescens*، نشاط مضاد للبكتيريا، البردجيوسين.

1. Introduction

Pseudomonas aeruginosa is a multi-drug resistance (MDR) opportunistic pathogen, aerobic, non-spore-forming, rod-shaped, and gram-negative bacteria that causes acute or chronic infections in immunocompromised individuals with chronic obstructive pulmonary disease (COPD), cystic fibrosis, cancer, traumas, burns, sepsis, and ventilator-associated pneumonia (VAP) [1–4]. Biofilm-formed *P. aeruginosa* may be able to endure hypoxia and other severe conditions [5]. The fast mutation and adaptability of *P. aeruginosa* to acquire resistance to antibiotics further complicate therapy [6]. Medical devices (ventilators) are a common source of *P. aeruginosa* since the bacteria thrive in moist environments. This makes them a leading cause of hospital-acquired illnesses [7]. Among the multidrug-resistant ESKAPE pathogens which include *E. faecium*, *S. aureus*, *K. pneumoniae*, *A. baumannii*, *P. aeruginosa*, and *E. coli*, *P. aeruginosa* is particularly noteworthy. The World Health Organisation classifies carbapenem-resistant *Pseudomonas aeruginosa* as a critical infection in need of new treatments immediately [8]. One of these organisms that produce prodigiosin pigment is *Serratia marcescens* which is a rod-shaped bacillus with a gram-negative reaction that belongs to the family Enterobacteriaceae [9, 10]. This pigment has antibacterial activity against *P. aeruginosa* [11, 12]. *P. aeruginosa* can cause infections such as lung infection, skin infection, and eyes of people with cystic fibrosis (CF), HIV/AIDS and burns and abrasions. These bacteria are ubiquitous microorganisms found in both natural and human-made environments, including those involving animals and plants. [1], [13–16]. Particles with a mean diameter of less than or equal to 100 nm and a high surface-to-volume ratio are known as nanoparticles (NPs). The visual features, catalytic activity, and antimicrobial capabilities of nanoparticles have garnered a lot of attention in recent years. There is a greater possibility of their use in fields like medicine, communications, and electronics because of their special qualities. Nanoparticles, endowed with these characteristics, have proven useful in a wide variety of industries [17]. Bactericidal activity against a wide variety of Gram-positive and -negative bacteria has been seen in iron oxide nanoparticles (NPs). NPs have been found to decrease *P. aeruginosa* biofilm and limit the development of *Escherichia coli* and *Staphylococcus aureus*. Degraded iron from the cores of iron oxide NPs seems to accumulate in the body's natural iron reserves, and the NPs themselves are non-toxic [18]. For these reasons, iron oxide nanoparticles are a promising new antibacterial treatment option. Consequently, the goal of the recent work was to determine whether or not nanoparticles of iron oxide synthesized with Ppodigiosin pigment from *Serratia marcescens* can suppress the growth of *P. aeruginosa*.

Previous Studies

Previous published studies laid down different methods of preparation and application. For example, a research was carried on to synthesize zinc oxide nanoparticles from prodigiosin dye to inhibit pseudomonas bacteria [19]. Another research was conducted to synthesize iron oxide from prodigiosin dye produced by the bacterium *Serratia* to inhibit the bacterium *Enterococcus faecalis* [20]. As for the current research, iron nanoparticles were created from

prodigiosin dye to inhibit pseudomonas bacteria. The nano sizes differed from one method of preparation to another.

2. Material and Method

Collection, Isolation and Identification of Clinical Specimens

A total of one hundred-twenty samples, obtained from burn and wound infections of different patients with ages between 15-25, included 70 samples from males and 50 from the females. All samples were subjected to various examinations including microscopic examination (gram staining), cultural characteristics (MacConkey agar, blood agar, *Pseudomonas* agar, and cetrimide agar) and biochemical tests (catalase, oxidase, indole, Simmons citrate, and urease tests) to isolate and identify isolates of *Pseudomonas aeruginosa* [21] [22].

In addition, 40 samples were collected from the soil to isolate *Serratia marcescens* by confirming its species using the VITEK-2 system.

Extraction and Purification of Prodigiosin Pigment

After 72 hours of incubation, the cell-free broth culture of *S. marcescens* yielded 250 ml of raw prodigiosin. The culture medium was centrifuged at 8000 rpm for 15 minutes. After removing the supernatant, 250 ml of methanol was added to the collected cells which was then stirred for 3 hours at room temperature. After 20 minutes of centrifugation at 8000 rpm, the resultant mixture was filtered using 0.2 m Whitman filter paper. The methanol filtrate was heated to 40°C in a rotary evaporator, and then twice as much chloroform was added to it to extract the red pigment [20].

Synthesis of Iron Oxide Nanoparticles

Prodigiosin pigment was produced by biosynthesising iron oxide (Fe_2O_3) nanoparticles. The prodigiosin pigment was prepared by adding 5 milligrams of prodigiosin powder to 50 millilitres of deionized distilled water (DDW) and dispersing the mixture with an ultrasonic bath for 30 minutes. The pigment was then mixed with 5 milligrams of ferric sulphate in 50 millilitres of the previously prepared pigment by shaking the flask in a darkroom overnight at room temperature. The combination was then centrifuged at 5000 rpm for 10 minutes. The prodigiosin pigment was washed twice with deionized distilled water from the precipitate of a solution containing the entire iron oxide (Fe_2O_3) nanoparticles. The nanoparticles were dried in a 40 degrees Celsius oven overnight after they had precipitated. Finally, a dark container was placed over the brown powder [20].

Characterization of Iron Oxide Nanoparticles

Different techniques were utilized to characterize iron oxide nanoparticles, including ultra-violate visible light (UV-Vis), atomic force microscopy (AFM), X-ray diffraction (XDR) analysis, fourier transforms infrared (FTIR) spectroscopy and field emission scanning electron microscopy (FE-SEM) [19].

Antibiotic Susceptibility Test

Several antibiotics were utilized to estimate the multi-drug resistance isolate of *P. aeruginosa*. Antibiotics (symbol, µg) utilized were: tobramycin (TOB, 10 µg), piperacillin-tazobactam (PIT, 100/10 µg), meropenem (MEM, 10µg), azithromycin (AT, 30µg), ceftazidime (CAZ, 30 µg), piperacillin (PRL, 100 µg), ofloxacin (OF, 5 µg), levofloxacin (LE, 5 µg), gentamicin (CN, 10 µg) and imipenem (IPM, 10 µg) according to CLSI, (2022) [23], and the results were represented as resistance, intermediate and sensitive.

Antibacterial Test

The agar well diffusion technique was used to determine the minimum inhibitory concentration (MIC) of biologically generated iron oxide NPs for their antibacterial properties against Gram-negative *P. aeruginosa* [24]. In this case, 25 ml of sterile medium made from Müller Hinton agar, was poured into pre-cleaned Petri dishes and left to set overnight in a lab. The agar medium with the grown test species was expanded using the sterile cotton swab method. As a result, solutions of varying concentrations of iron oxide NPs (6.25,12.5,25, 50, 100, 200 mg/ml) were introduced into the previously drilled wells. The plates were then placed in incubator at 37^{o}C for 24 hours and then the inhibition zone size was calculated for each well [19].

3. Results and Discussion

Collection, Isolation and Identification of Bacterial Samples

One hundred twenty samples were collected from burn and wound infections of different patients of different ages and sexes. All samples were subjected to various examinations. Firstly, *P. aeruginosa* cells were given a negative gram reaction that appeared as single bacterial cells arranged in small pairs, rods. The cultural characteristics of *P. aeruginosa* were determined on MacConkey and cetrimide agars. On MacConkey, colonies of this bacterium appeared as pale colour shape as *P. aeruginosa* was a non-lactose fermented bacterium, while greenish-yellow colour colonies of this bacterium appeared on cetrimide agar medium due to the ability of *P. aeruginosa* to survive with the toxic cetrimide material (Figure 1).

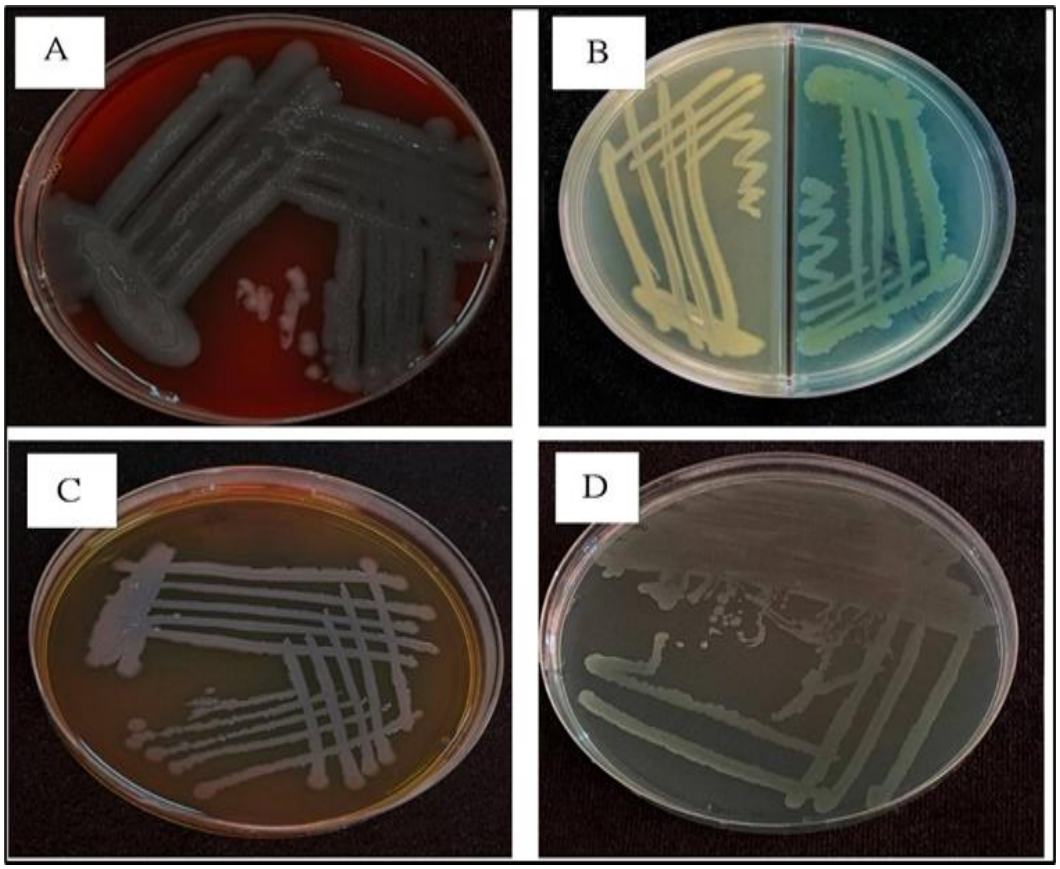

Figure 1: Colonies of *P. aeruginosa* on: A: Blood agar, B: Cetrimide agar, C: MacConkey agar and D: *Pseudomonas* agar.

Several biochemical tests were performed to confirm that the isolates were *P. aeruginosa*. The results of all isolates investigated are shown in Table 1.

Table 1: The biochemical tests of *P. aeruginosa*.

Test	Result
Oxidase	+
Catalase	+
Indole Test	-
Simmons Citrate Test	+
Urease Test	+

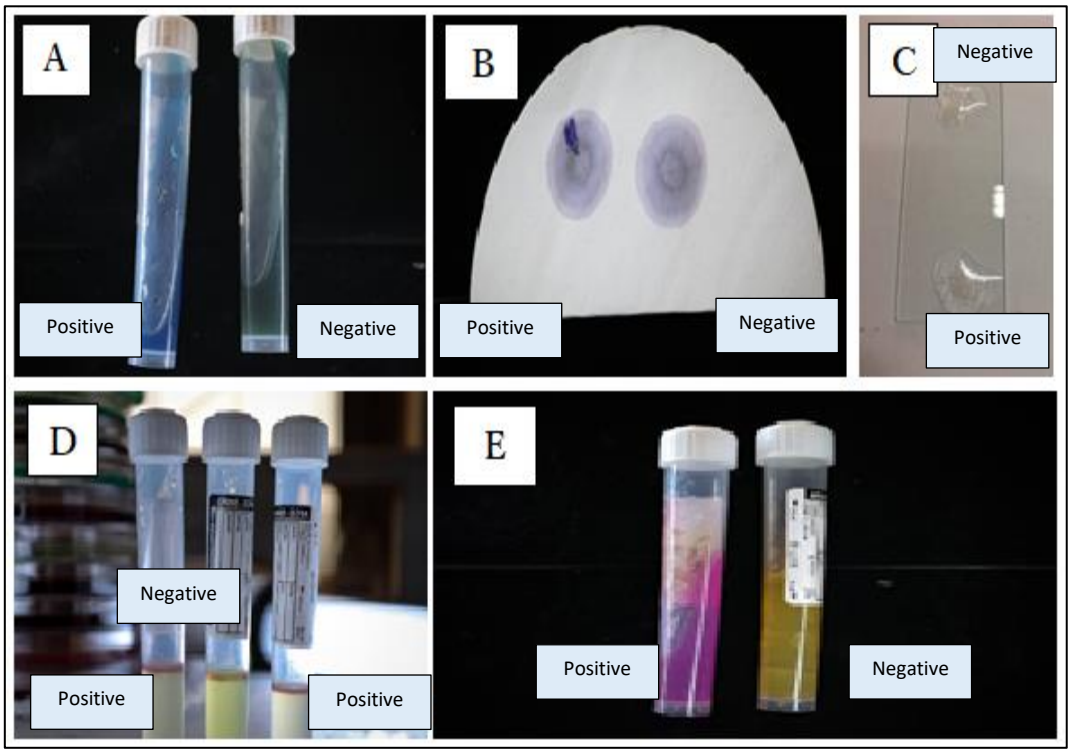

Figure 2: Biochemical tests for Identification of bacterial isolate, (A): Simmons Citrate test, (B): Oxidase test, (C): Catalase test, (D): Indol test, (E): Urease test**.**

Furthermore, the red-pigmented colonies of *S. marcescens* were cultured on nutrient agar (Figure 3), whereas the isolate of *Serratia marcescens* was utilized to produce prodigiosin pigment after performing the VITEK-2 system (Figure 4):

Figure 3: *Serratia marcescens* on nutrient agar.

Comments:	

Identification Information	Analysis Time:	3.97 hours	Status:	Final
Selected Organism	99% Probability	Serratia marcescens		
	Bionumber:	6125711455006210		
ID Analysis Messages				

Biochemical Details																
2	APPA	-	3	ADO	+	4	PyrA	+	5	lARL	+	7	dCEL	-	9	BGAL	-
10	H2S	-	11	BNAG	+	12	AGLTp	-	13	dGLU	+	14	GGT	-	15	OFF	+
17	BGLU	+	18	dMAL	+	19	dMAN	+	20	dMNE	+	21	BXYL	-	22	BAlap	-
23	ProA	+	26	LIP	-	27	PLE	-	29	TyrA	-	31	URE	-	32	dSOR	+
33	SAC	+	34	dTAG	-	35	dTRE	+	36	CIT	+	37	MNT	-	39	5KG	+
40	lLATk	-	41	AGLU	-	42	SUCT	-	43	NAGA	-	44	AGAL	-	45	PHOS	-
46	GlyA	-	47	ODC	+	48	LDC	+	53	lHISa	-	56	CMT	+	57	BGUR	-
58	O129R	+	59	GGAA	-	61	lMLTa	-	62	ELLM	-	64	lLATa	-			

Figure 4: VITEK 2 system of *Serratia marcescens*.

Production of Prodigiosin Pigment

Prodigiosin production started after 72 hours in the shaker incubator. Prodigiosin concentrations were around 0.71 g/L (after four runs) towards the conclusion of the exponential phase (after 48 hrs. of incubation) and peaked at 0.83 g/L (after 45 hrs. of incubation) during the stationary phase. After the exponential phase (after 48 hours of incubation), the concentration of prodigiosin was around 0.71 g/L (after four runs), and it peaked at 0.83 g/L after 45 hours in the shaker incubator, during the stationary phase. As prodigiosin was produced and accumulated mostly during the stationary phase of the

incubation, the medium changed its colour from yellow to red [20]. Figure 5 shows the prodigiosin pigment in the production medium.

Figure 5: Prodigiosin pigment in the production medium.

Characterization of Prodigiosin Pigment

Maximum absorption of *Serratia marcescens* prodigiosin pigment was measured using a UV-visible spectrophotometer (Shimadzu, Japan). Absorption was evaluated at 534 nm(Figure 6). This result was close to the result obtained by Yaaqoob [20], where he evaluated the absorption at 529 nm.

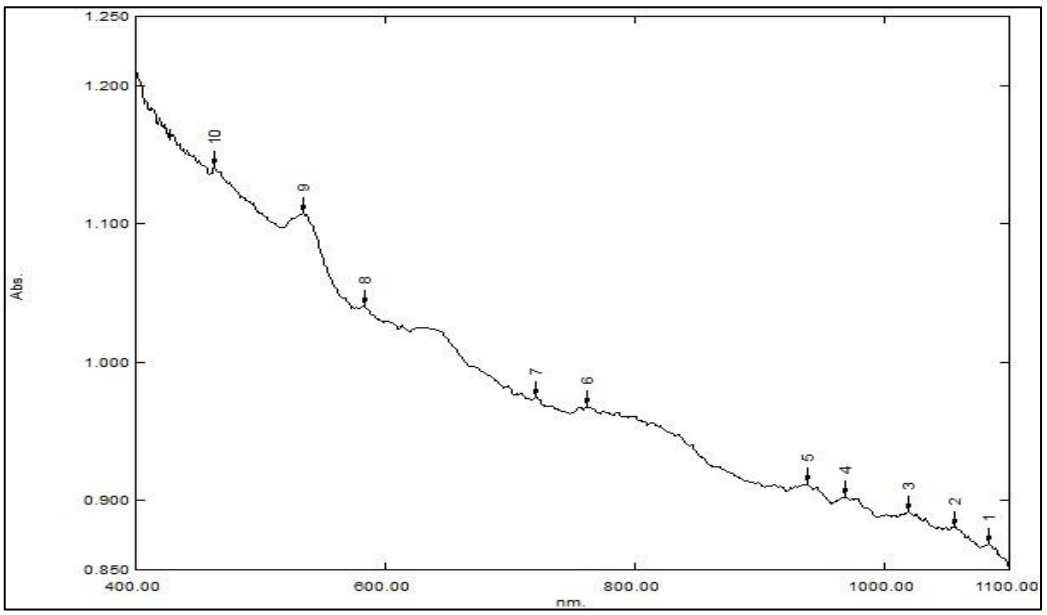

Figure 6: Absorption pattern of purified pigment, isolated from *Serratia* sp. Absorbance was measured at 534 nm.

Ultra-violate Visible Light (UV-Vis) Investigation for Iron Oxide NPs

The optical characteristics of the biosynthesized iron nanoparticles were studied utilizing the UV-Vis spectroscopy method. The attained result showed a pronounced UV absorption at around 200 nm (Figure 7).

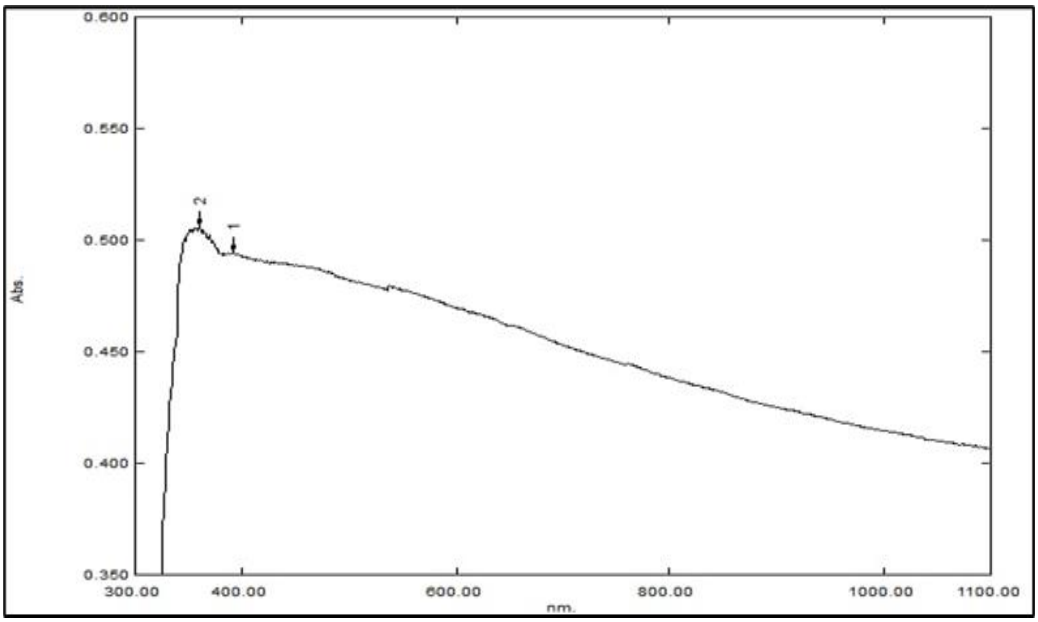

Figure 7: Spectrum of UV-Vis of the iron oxide NPs.

Atomic Force Microscopy (AFM) Investigation

It was first used to examine the properties of the surface of iron oxide nanoparticles in 2D and 3D. The results of the atomic force microscope analysis showed that the iron oxide nanoparticles were round and had an average diameter of 50.73 nm (Figure 8). In general, this findings in corresponding with Yaaqoob's [20], who reported that diameter of these NPs was around 35.01nm

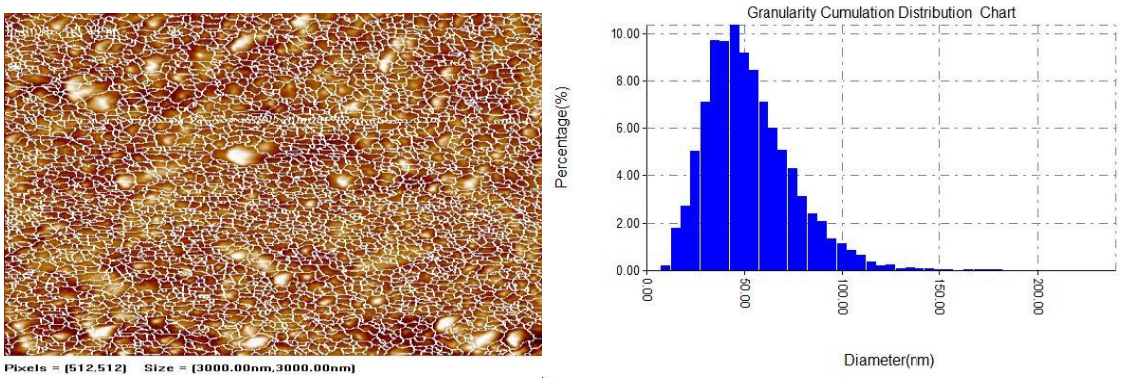

Figure 8: Atomic Force Microscopy of iron oxide NPs (A: Histogram of iron oxide NPs, B: 2D and 3D of iron oxide nanoparticles).

Avg. Diameter: 50.73 nm	<=10% Diameter: 25.00 nm
<=50% Diameter: 45.00 nm	<=90% Diameter: 80.00 nm

X-ray Diffraction (XRD) Investigation

The XRD investigation of the iron oxide NPs produced biologically (Figure 9). Throughout observation, three distinct peaks were seen at 2θ = 11.9867º, 19.9940º and 22.5561º. The Debye-Scherrer equation was used to determine the crystalline particles' sizes in the meantime:

$$D = \left[\frac{K\lambda}{\beta\cos\theta}\right] A^o$$

In this equation, D stands for the crystallite size, K represents the form factor which is a constant (0.9), and λ stands for the x-ray wavelength (1.5406 A^o). Nanoparticles' Bragg angles and corrected line broadening are denoted by θ and β respectively.

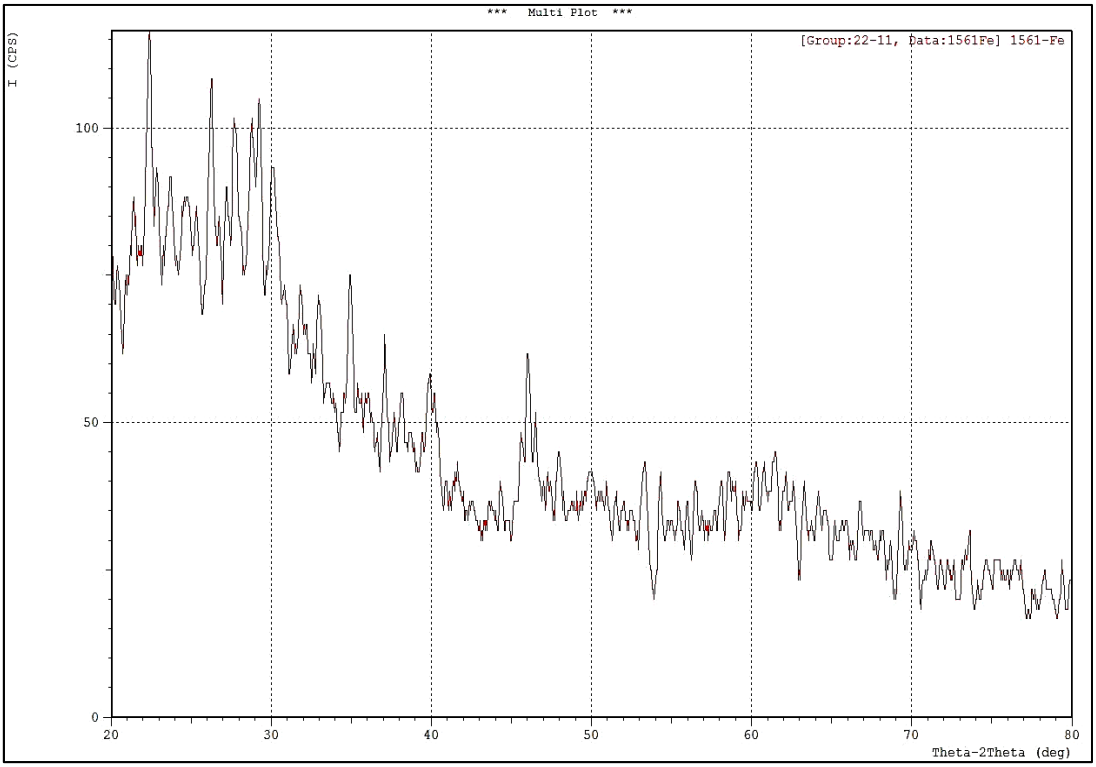

Figure 9: XRD patterns of the bio-synthesized iron NPs.

Fourier Transforms Infrared (FTIR) Spectroscopy Analysis

Figures 10 and 11 display the FT-IR data for the iron oxide NPs produced via biosynthesis. A succession of absorption peaks between 400 and 4000 cm^{-1} was frequently noticed which corresponded to hydroxyl and carboxylate groups in the substance. In particular, the C-Harmonics stretching mode is responsible for a broad frequency range of about 3415.70 cm^{-1}. The N-O (Nitro compounds) stretching vibration is responsible for the majority of the other peaks around 1419.51 cm^{-1}. In addition, the C-C (in-ring) aromatics stretching mode is responsible for the peak observed at 1575.73 cm^{-1}. This result was consistent with thefindings by Alden and
Yaaqoob [19].

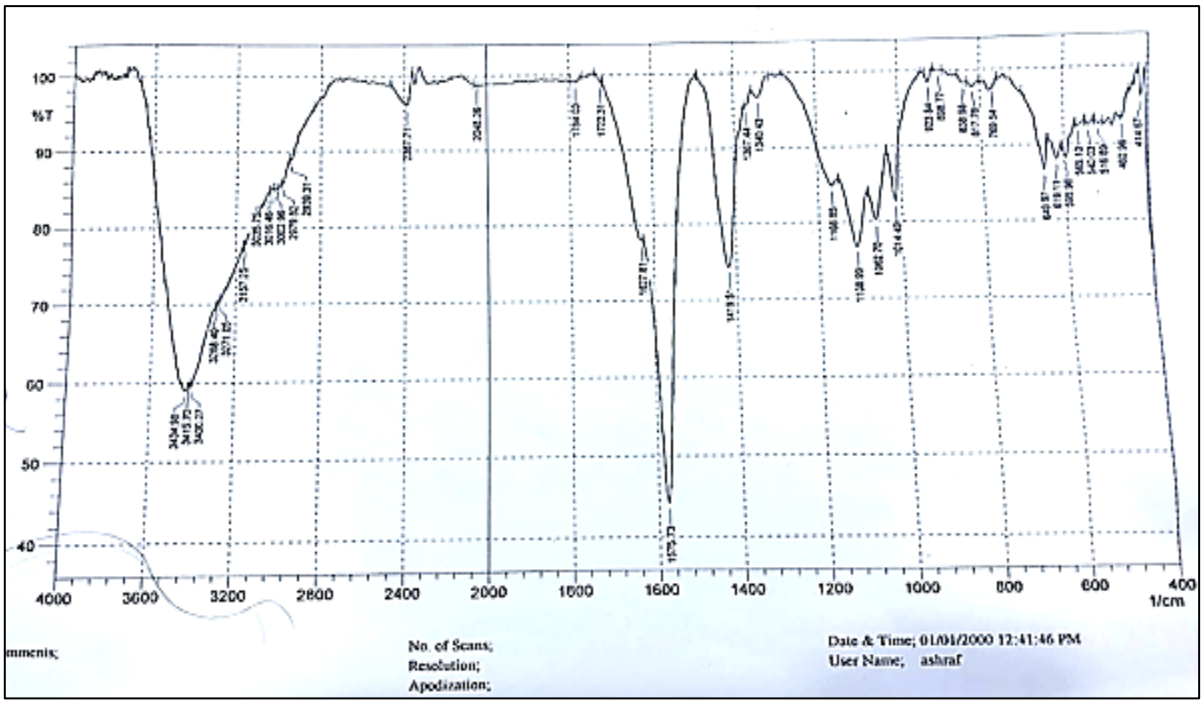

Figure 10: FT-IR spectrum of the biosynthesized iron oxide nanoparticles.

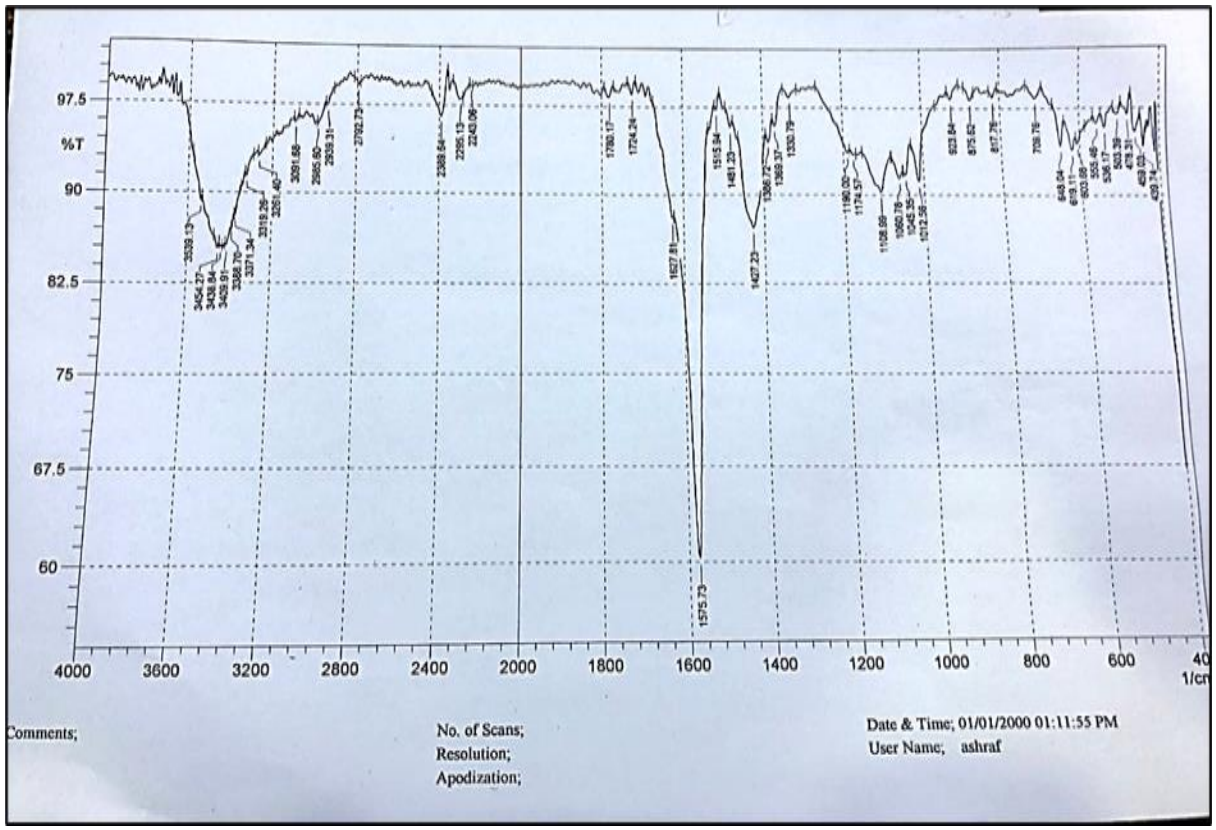

Figure 11: FT-IR spectrum of the biosynthesized iron oxide NPs and Prodigiosin pigment.

Table :2 FTIR of Fe_2O_3 nanoparticles

Compound Type	Frequency Absorption(cm^{-1})	Bonds	Compound Class of Functional Groups
Prodigiosin	3427.27-3415.91	O-H stretching	Alcohol
	2387.71	S-H stretching	Thiol
	1575.73	N-O stretching	Nitro Compound
	1417.58	S=O stretching	Sulphate
(Fe_2O_3:) NPs	3323.12 -3284.55	N-H stretching	Aliphatic primary amine
	2960.53-2925.81	C-H stretching	Alkane
	1649.02-1629.74	C=C stretching	Alkene
	1400.22	C-F stretching	Fluoro Compound
	1095.49	C-O stretching	Secondary Alcohol
	1022.49	C-N stretching	Amine
	675.04	C-Br stretching	Halo Compound

Field Emission Scanning Electron Microscopy (FE-SEM) Analysis

The FE-SEM method was used to investigate the morphological characteristics of the biosynthesized iron oxide NPs. Particles of a spherical shape were seen in the iron oxide NPs sample that had been synthesized (Figure 12).

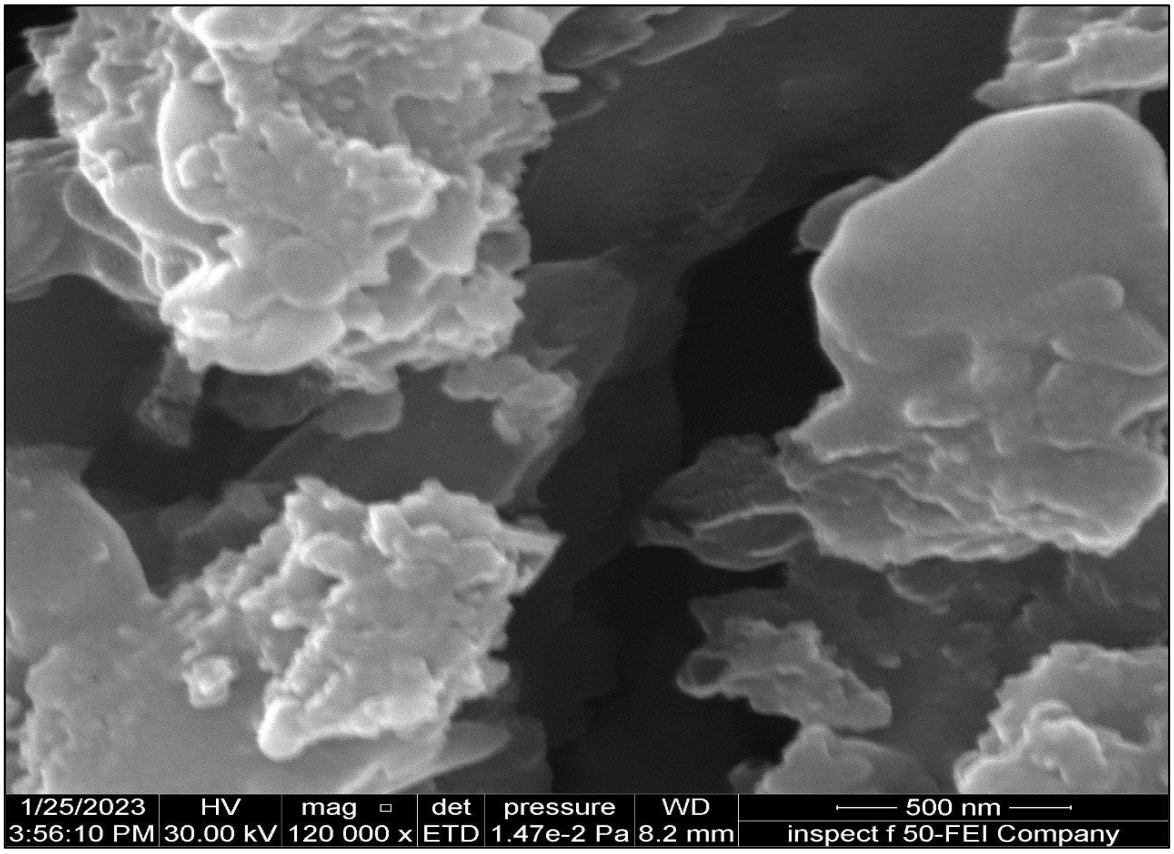

Figure 12: Images of the biosynthesized iron oxide NPs using FE-SEM.

Antibiotics Susceptibility Test:

Antibiotics utilized to estimate the multi-drug resistance isolate of *P. aeruginosa* were: tobramycin (TOB), piperacillin-tazobactam (PIT), meropenem (MEM), azithromycin (AT), ceftazidime (CAZ), piperacillin (PRL), ofloxacin (OF), levofloxacin (LE), gentamicin (GN)

and imipenem (IPM) according to CLSI 2022 [23], and the results were represented as resistance, intermediate and sensitive.

Based on the results, majority of isolates were resistant to MEM, TOB, PIT, AT and GN. While rest of these isolates showed intermediate resistance against CAZ, PRL, OF and LE.
The growth and spread of multidrug-resistant (MDR) strains of *P. aeruginosa* has been considered a major health problem for many reasons and is a leading cause of death from infection, especially in hospitals and among those with impaired immune systems. It can be selectively favoured and disseminate antimicrobial resistance *in vivo* to an extraordinary degree. The rapid and widespread dissemination of high-risk *P. aeruginosa* clones is a hazard to global public health that must be investigated and addressed with haste and resolve [25].

The multi-drug resistant isolate of *P. aeruginosa* was selected for further experiments, after performing VITEK2-system which ensured that this isolate was *P. aeruginosa* (Figures 13 and 14):

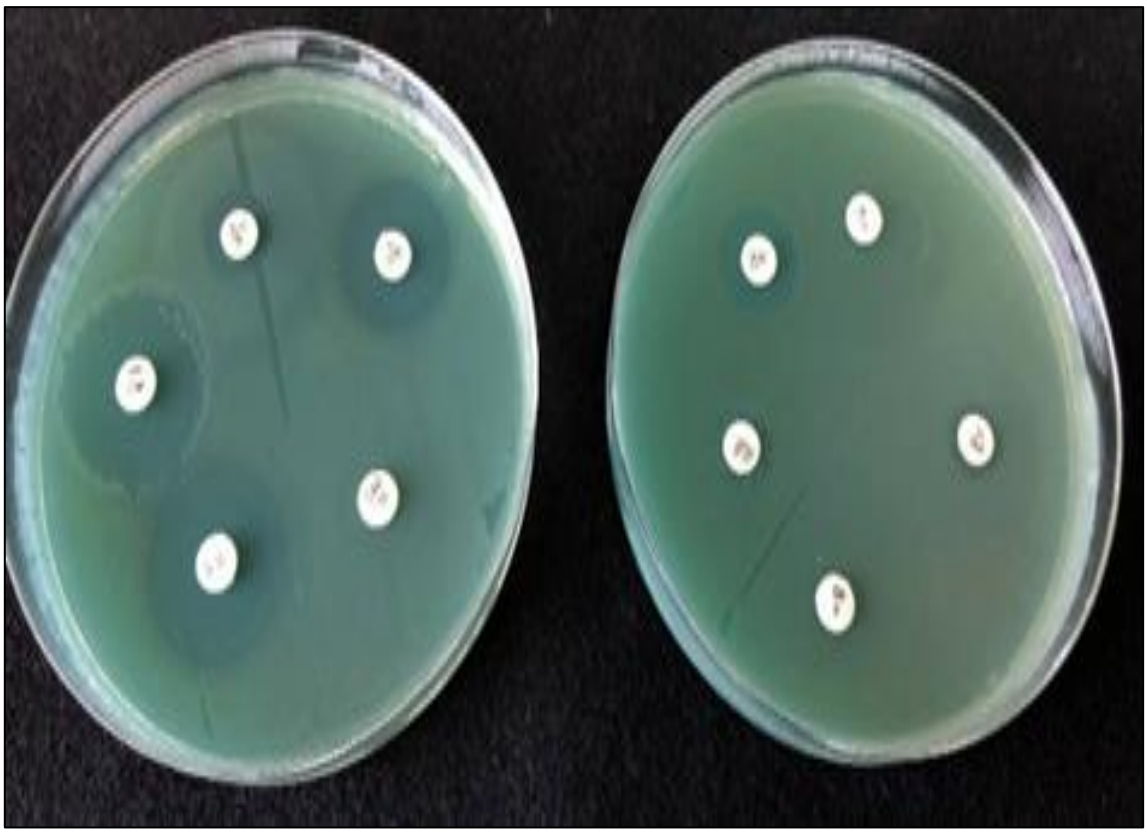

Figure 13: Antibiotic test of *P. aeruginosa*.

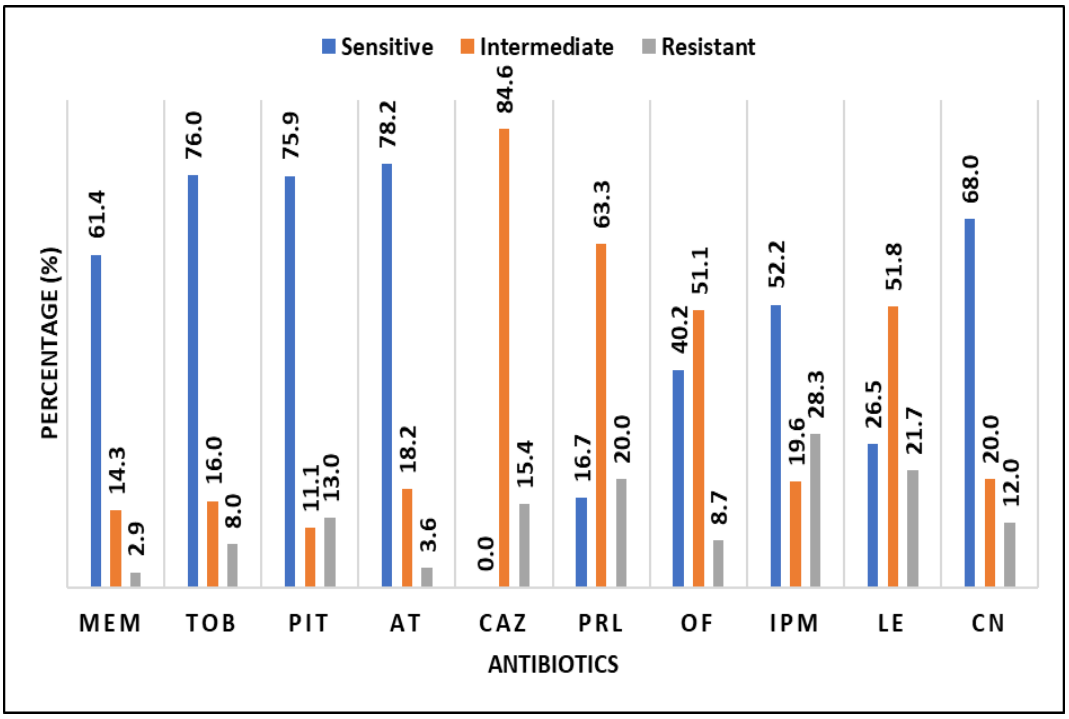

Figure 14: Antibiotics susceptibility test of *P. aeruginosa*.

bioMérieux Customer: Microbiology Chart Report Printed December 13,2022 8:22:25 AM AST
Patient Name: Bakr,. Patient ID:XCVXCB CX
Location: Physician:
Lab ID:141 Isolate Number:1
Organism Quantity:
Selected Organism:Pseudomonas aeruginosa
Source: Collected:

Comments:	

Identification Information	Analysis Time: 8.00 hours	Status: Final
Selected Organism	Pseudomonas aeruginosa Bionumber: 0003051103500352	
ID Analysis Messages		

Biochemical Details

2	APPA	-	3	ADO	-	4	PyrA	-	5	1ARL	-	7	dCEL	-	9	BGAL	-
10	H2S	-	11	BNAG	-	12	AGLTp	-	13	dGLU	+	14	GGT	+	15	OFF	-
17	BGLU	-	18	dMAL	-	19	dMAN	-	20	dMNE	┼	21	BXYL	-	22	BAlap	+
23	ProA	┼	26	LIP	(-)	27	PLE	-	29	TyrA	+	31	URE	-	32	dSOR	-
33	SAC	-	34	dTAG	-	35	dTRE	-	36	CIT	+	37	MNT	+	39	5KG	-
40	ILATk	┼	41	AGLU	-	42	SUCT	┼	43	NAGA	-	44	AGAL	-	45	PHOS	-
46	GlyA	-	47	ODC	-	48	LDC	-	53	1HISa	+	56	CMT	+	57	BGUR	-
58	O129R	┼	59	GGAA	-	61	IMLTa	┼	62	ELLM	-	64	ILATa	┼			

Figure 15: VITEK 2 system result of *P. aeruginosa*.

Antibacterial Test:

The Fe_2O_3 NPs were tested for their ability to inhibit the growth of gram-negative bacteria (*Pseudomonas aeruginosa*). The MIC of Fe_2O_3 NPs against several bacteria was determined using the agar well diffusion method [26]. Almost 25 grams of the sterile Mueller Hinton agar medium was poured onto sterile plates and was then allowed to harden at room temperature. A sterile cotton swab was used to transfer the test organism's growth to the agar medium and distribute it evenly throughout the surface. Next, several Fe_2O_3 NPs concentrations (6.25, 12.5, 25, 50, 100, and 200 mg/ml) were prepared. Fe_2O_3 NP-inoculated plates were kept at 37°C for 24 hours, and then the inhibition zone surrounding each well was measured [20].

The outcomes of the antibacterial activity of Fe2O3 NPs can be seen in Figure 16. The concentration of Fe_2O_3 NPs had a linear relationship with the antibacterial activity. At a dosage of 200 mg/ml of Fe_2O_3 NPs, the maximum inhibition zone surrounding a *P. aeruginosa* isolate was 27 mm; while at a concentration of 25 mg/ml, the lowest inhibition zone was 14 mm. The susceptibility of the bacteria utilized in this investigation may account for the observed variation in inhibition diameter caused by various interactions between Fe_2O_3 NPs and the microorganism. Since microorganisms have negative charges, the main mechanism of toxicity of Fe_2O_3 NPs associated with metal oxides is electromagnetic interaction between microorganisms and metal oxides which leads to oxidation and, ultimately, death of microorganisms.

Fe_2O_3 nanoparticlesbactericidal effect on bacteria is of utmost relevance as dangerous bacteria may even enter the food chain. Recent studies have shown that Fe_2O_3 has an antibacterial impact on bacteria and fungi, and this information is being communicated to the scientific community [20]. Nanoparticles made of metal oxides have recently been shown to exhibit powerful antibacterial capabilities, similar to those of noble elements. These inorganic nanomaterials inhibit bacterial growth by modifying membrane charges, releasing ions, lowering ATP synthesis, and producing reactive oxygen species (ROS), among other mechanisms. The functional and structural integrity of the bacterial cell is compromised as a result of the combined effects of ROS generated in the cellular environment and the aforementioned processes which act on proteins, nucleic acids (DNA, RNA), the cell wall, and the plasma membrane. The bactericidal activity and range of inorganic nanoparticles are both boosted by the fact that they use several, non-specific mechanisms to harm bacteria [27]. Prodigiosin, which was shown to have bactericidal and bacteriostatic actions against several bacteria including *P. aeruginosa*, may also be responsible for this antimicrobial activity [28].

Table 3: Antibacterial activities of the biosynthesized iron oxide NPs against *P. aeruginosa* at concentrations of 1) 200µg/ml, 2) 100µg/ml, 3) 50µg/ml, 4) 25µg/ml, 6) 12.5µg/ml and 7) 6.25µg/ml.

No.	Con. (µg/ml)	Fe Nanoparticles Zone of Diameter (mm)
1	200	24
2	100	23
3	50	19
4	25	10
5	12.5	No inhibition zone
6	6.25	No inhibition zone

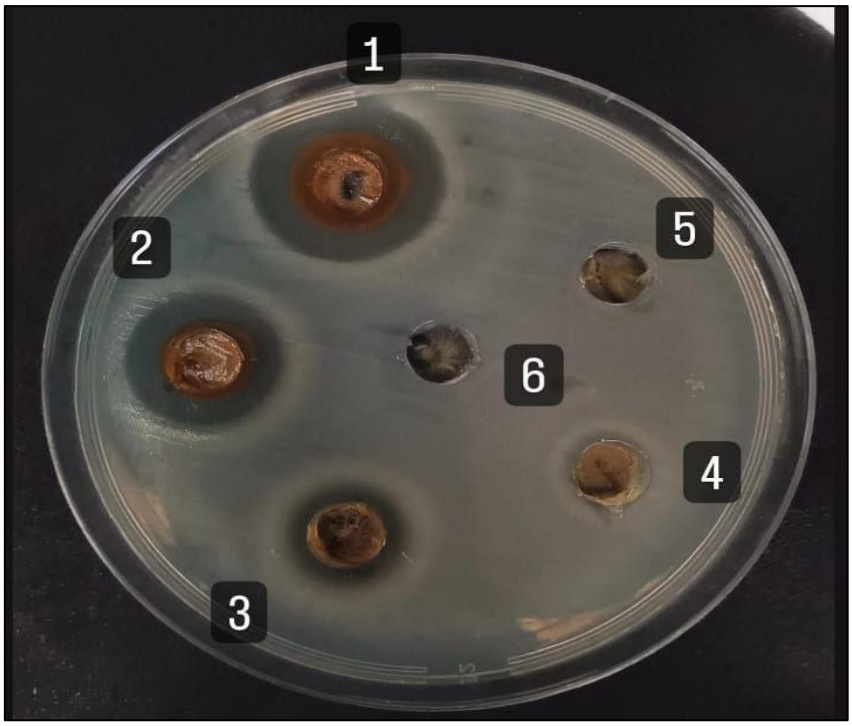

Figure 16: Antibacterial activity of (Fe_2O_3) nanoparticles on *Pseudomonas aeruginosa*.

4. Conclusion

Iron oxide nanoparticles that loaded on prodigiosin showed effective antibacterial activity against *P. aeruginosa*. It was clearly noticed that the Fe_2O_3NPs antibacterial activity was immediately dependent on the utilized concentrations.

5. Ethical Clearance

The experiments described in this study were approved by the Biotechnology Department's local committee. The research was conducted by a group from the University of Baghdad.

6. Conflict of Interest

The authors have no conflicts of interest to declare.

References:

[1] B. Rudra and R. S. Gupta, "Phylogenomic and comparative genomic analyses of species of the family Pseudomonadaceae: Proposals for the genera Halopseudomonas gen. nov. and Atopomonas gen. nov., merger of the genus Oblitimonas with the genus Thiopseudomonas, and transfer of some misclassified species of the genus Pseudomonas into other genera," *Int J Syst Evol Microbiol*, vol. 71, no. 9, p. 005011, 2021.

[2] A. D. Salman, Z. Amer, and E. S. Abud-Rahman, "Bacteriological study Bacteriological study of Pseudomonas aeruginosa isolated from different infections and study antimicrobial activities of plant extract Solanum nigrum against it," *Iraqi Journal of Science*, pp. 2278–2284, 2017.

[3] E. Rossi *et al.*, "Pseudomonas aeruginosa adaptation and evolution in patients with cystic fibrosis," *Nat Rev Microbiol*, vol. 19, no. 5, pp. 331–342, 2021.

[4] E. G. Sweedan, "The Antimicrobial Effects of Alcoholic Leaves Extract of Salvia Officinalis Against Multidrug Resistant Pseudomonas Aeruginosa," *Iraqi Journal of Science*, pp. 441–448, 2021.

[5] M. Sinha *et al.*, "Pseudomonas aeruginosa theft biofilm require host lipids of cutaneous wound," *Ann Surg*, vol. 277, no. 3, pp. e634–e647, 2023.

[6] K. C. Blomquist and D. E. Nix, "A critical evaluation of newer β-lactam antibiotics for treatment of Pseudomonas aeruginosa infections," *Annals of Pharmacotherapy*, vol. 55, no. 8, pp. 1010–1024, 2021.

[7] M. H. AlMamoory and I. K. Al-Mayaly, "Biodegradation of Cypermethrin by Two Isolates of Pseudomonas aeruginosa," *Iraqi Journal of Science*, pp. 2309–2321, 2017.

[8] I. Q. Mohamed and H. R. R. Al-Taai, "Phylogenetic Analysis of Klebsiella pneumoniae Isolated from Nosocomial and Community Infection in Diyala, Iraq," *Iraqi Journal of Science*, pp. 2726–2740, 2023.

[9] D. Prabhu, S. Rajamanikandan, S. B. Anusha, M. S. Chowdary, M. Veerapandiyan, and J. Jeyakanthan, "In silico functional annotation and characterization of hypothetical proteins from Serratia marcescens FGI94," *Biology Bulletin*, vol. 47, pp. 319–331, 2020.

[10] H. K. Abid, "The Effect of Prodigiosin Extracted from Serratia marcescens on DNA Fragmentation of Human Peripheral Blood Lymphocytes Cells," *Iraqi Journal of Science*, vol. 56, no. 2C, pp. 1661–1666, 2015.

[11] A. Derakhshanfar, B. Rastegari, H. Sharifi, H. Khajeh-Zadeh, and J. Moayedi, "The effectiveness of antimicrobial photodynamic therapy with prodigiosin against reference strains of Staphylococcus aureus, Escherichia coli, and Pseudomonas aeruginosa," *Lasers Med Sci*, vol. 37, no. 9, pp. 3631–3638, 2022.

[12] L. A. Yaaqoob, R. W. Younis, Z. K. Kamona, M. F. Altaee, and R. M. Abed, "Biosynthesis of Nio Nanoparticles Using Prodigiosin Pigment and its Evaluate of Antibacterial Activity Against Biofilm Producing MDR-Pseudomonas Aeruginosa," *Iraqi Journal of Science*, pp. 1171–1179, 2023.

[13] S. J. Wood, T. M. Kuzel, and S. H. Shafikhani, "Pseudomonas aeruginosa: Infections, Animal Modeling, and Therapeutics," *Cells*, vol. 12, no. 1, p. 199, 2023.

[14] M. Jayaprakashvel, M. Sami, and R. Subramani, "Antibiofilm, antifouling, and anticorrosive biomaterials and nanomaterials for marine applications," *Nanostructures for Antimicrobial and Antibiofilm Applications*, pp. 233–272, 2020.

[15] R. A. K. AL-Fridawy, W. A. H. Al-Daraghi, and M. H. Alkhafaji, "Isolation and Identification of Multidrug Resistance Among Clinical and Environmental Pseudomonas aeruginosa Isolates," *Iraqi journal of biotechnology*, vol. 19, no. 2, 2020.

[16] W. Al-Daraghi, I. T. Lafta, and F. H. Al-Hamedi, "Isolation and Identification of lipA Gene Producing Pseudomonas aeruginosa from Industrial Wastewater," *Iraqi journal of biotechnology*, vol. 18, no. 1, 2019.

[17] N. Shabani, A. Javadi, H. Jafarizadeh-Malmiri, H. Mirzaie, and J. Sadeghi, "Potential application of iron oxide nanoparticles synthesized by co-precipitation technology as a coagulant for water treatment in settling tanks," *Min Metall Explor*, vol. 38, pp. 269–276, 2021.

[18] L. M. Armijo *et al.*, "Antibacterial activity of iron oxide, iron nitride, and tobramycin conjugated nanoparticles against Pseudomonas aeruginosa biofilms," *J Nanobiotechnology*, vol. 18, no. 1, pp. 1–27, 2020.

[19] M. A. A. Alden and L. A. Yaaqoob, "EVALUATION OF THE BIOLOGICAL EFFECT SYNTHESIZED ZINC OXIDE NANOPARTICLES ON PSEUDOMONAS AERUGINOSA," *IRAQI JOURNAL OF AGRICULTURAL SCIENCES*, vol. 53, no. 1, pp. 27–37, 2022.

[20] L. A. Yaaqoob, "Evaluation of the biological effect synthesized iron oxide nanoparticles on Enterococcus faecalis," *IRAQI JOURNAL OF AGRICULTURAL SCIENCES*, vol. 53, no. 2, pp. 440–452, 2022.

[21] D. N. Faraj and O. J. Mohammed, "Detection of Extended Spectrum β-lactamases and Metallo β-lactamases in Pseudomonas Aeruginosa isolated from Burns".

[22] N. N. Hussein and A. H. Muslim, "Detection of the antibacterial activity of AgNPs biosynthesized by Pseudomonas aeruginosa," *The Iraqi journal of agricultural science*, vol. 50, no. 2, pp. 617–625, 2019.

[23] A. Shamsheyeva *et al.*, "2144. Performance of 2019 CLSI Ciprofloxacin Breakpoint Antimicrobial Susceptibility Testing Algorithms for Enterobacteriaceae and Pseudomonas aeruginosa Directly from Positive Blood Culture on the Accelerate Pheno™ System.," in *Open forum infectious diseases*, 2019.

[24]P. K. Stoimenov, R. L. Klinger, G. L. Marchin, and K. J. Klabunde, "Metal oxide nanoparticles as bactericidal agents," *Langmuir*, vol. 18, no. 17, pp. 6679–6686, 2002.

[25]J. P. Horcajada *et al.*, "Epidemiology and treatment of multidrug-resistant and extensively drug-resistant Pseudomonas aeruginosa infections," *Clin Microbiol Rev*, vol. 32, no. 4, pp. e00031-19, 2019.

[26]I. Machado, J. Graça, H. Lopes, S. Lopes, and M. O. Pereira, "Antimicrobial pressure of ciprofloxacin and gentamicin on biofilm development by an endoscope-isolated Pseudomonas aeruginosa," *Int Sch Res Notices*, vol. 2013, 2013.

[27]M. Bhushan, D. Mohapatra, Y. Kumar, and A. K. Viswanath, "Fabrication of novel bioceramic α-Fe2O3/MnO nanocomposites: study of their structural, magnetic, biocompatibility and antibacterial properties," *Materials Science and Engineering: B*, vol. 268, p. 115119, 2021.

[28]A. Derakhshanfar, B. Rastegari, H. Sharifi, H. Khajeh-Zadeh, and J. Moayedi, "The effectiveness of antimicrobial photodynamic therapy with prodigiosin against reference strains of Staphylococcus aureus, Escherichia coli, and Pseudomonas aeruginosa," *Lasers Med Sci*, vol. 37, no. 9, pp. 3631–3638, 2022.